# F02

*Proceedings of the 5th International Conference on Inverse Problems in Engineering: Theory and Practice, Cambridge, UK, 11-15th July 2005*

## A NEW ENTROPY-BASED STRATEGY FOR THE INVERSE DESIGN OF A RADIO INTERFEROMETRIC ARRAY

C. FARIA[1], S. STEPHANY[2] and H. S. SAWANT[3]
[1]*Department of Computer Science, PUCMINAS, Poços de Caldas, MG, Brazil*
e-mail: faria@pucpcaldas.br
[2]*Computing and Applied Mathematics Lab (LAC), INPE, São José dos Campos, SP, Brazil*
e-mail: stephan@lac.inpe.br
[3]*Astrophysics Division, INPE, São José dos Campos, SP, Brazil*
e-mail: sawant@das.inpe.br

**Abstract -** Radio interferometric arrays measure the Fourier transform of the sky brightness distribution in a finite set of points that are determined by the cross-correlation of the different pairs of antennas in the array. The sky brightness distribution is reconstructed by the inverse Fourier transform of the sampled visibility. The quality of the reconstructed images strongly depends on the array configuration, since it determines the sampling function. This work proposes a new optimization strategy for the array configuration that is based on the entropy of the response function in both the Fourier and spatial domains. A stochastic optimizer, the Ant Colony System, employs entropy information to iteratively refine the candidate solutions. The proposed strategy was developed for the Brazilian Decimetric Array, a radio-interferometric array that is currently being developed for solar observations at the Brazilian Institute for Space Research (INPE). Configurations results for an optimized configuration are presented and compared to the results obtained using a standard configuration approach.

### 1. INTRODUCTION

A radio interferometric array measures the Fourier transform of the sky brightness distribution in a finite set of points that are determined by the cross-correlation of the different pairs of antennas in the array. Each pair measures a specific Fourier component, according to the distance between the antennas, the frequency of observation and incident angle. The sky brightness distribution is reconstructed by the inverse Fourier transform of the sampled visibility, i.e. the set of sampled points. The quality of the reconstructed images strongly depends on the array configuration, since it determines the sampling function. The optimization of the array configuration has exponential complexity. Several strategies are found in the literature [1-3] in order to improve the quality of the final image. This work proposes a new optimization strategy for the array configuration that is based on the entropy of the response function in both the Fourier and spatial domains. A stochastic optimizer, the Ant Colony System, employs the entropy information to iteratively refine the candidate solutions. The criterion adopted for the optimization is to obtain a set of sampling points in the Fourier domain that provide a coverage as uniform and complete as possible for the given set of antennas. A further criterion for image quality is to obtain a beam with a narrow high-intensity main lobe and low-intensity side lobes from a point source in the zenith of the sky. The proposed strategy was developed in the scope of the Brazilian Decimetric Array, a radio-interferometric array that is currently being developed for solar observations at the Brazilian Institute for Space Research (INPE). Configuration results for an optimized configuration are presented and compared with those obtained using a standard approach. The resulting coverage in the Fourier domain, the beam corresponding to a point source (point spread function), and some simulations using Solar image data from the Nobeyama radioheliograph (Japan) are shown.

### 2. RADIO INTERFEROMETRY

A radio telescope is an instrument that allows observation of the radiation signal intensity generated by astronomical sources in the sky. It provides data related to the variation of the signal intensity in function of time, frequency and/or angular position of the source. The angular resolution of a radio telescope is given by:

$$R \approx \lambda / D \tag{1}$$

where $\lambda$ is the wavelength of the electromagnetic wave plane, and $D$ is the diameter of the antenna dish. In order to improve this resolution the diameter of the antenna must be increased. However, there are practical limitations to construct large dishes in radio astronomy. An alternative for improving this resolution is to use a radio interferometric array, which is composed of two or more radio telescopes that simultaneously observe the signal from astronomical sources. Henceforth, it will refer to each radio telescope of the radio interferometric array as being an antenna.

A radio interferometric array measures the Fourier transform of the sky brightness distribution, the source image $I(x,y)$, producing a set of points in the Fourier domain $(u,v)$ that can be expressed by the visibility function $V(u,v)$ defined as follows [4]:

$$V(u,v) = \int I(x,y) e^{-2\pi i(ux+vy)} dxdy \quad (2)$$

Each pair of antennas of the radio interferometric array measures the cross-correlation of the signals obtained from the entire source image producing a corresponding sampled point in the frequency domain. A radio interferometric array composed by N antennas measures N(N-1)/2 Fourier components of the radio source. The vector separation that joins a specific pair of antennas is called the *baseline*. The location of a sampled point in the Fourier plane measured by one interferometric pair is mainly determined by the projection of their *baseline* onto a plane that is normal to the direction of the incident radiation [4,5].

Theoretically, the measured visibility $V'(u,v)$ would allow to reconstruct the image of the source applying an inverse Fourier transform. However, in practice, the value of the visibility function $V(u,v)$ is only known in a few points of the Fourier plane. Since each pair of antennas produces a specific sample point of the visibility function, a finite array of antennas will provide a finite number of visibility sample points.

The measured visibility strongly depends on the array configuration given by the antenna locations, since it determines the sampling function of the Fourier plane, denoted by *S*. The sampling function may be expressed in terms of a two-dimensional characteristic function, defined as unity at the *k* sampled points $(u,v)$ where the visibility is measured by the array, and zero elsewhere.

$$S(u,v) = \sum_k \delta(u-u_k)\,\delta(v-v_k) \quad (3)$$

The set of points in the *uv* plane where the complex visibility is measured is commonly denoted of *uv* coverage. The measured visibility $V'(u,v)$ is defined by

$$V'(u,v) = S(u,v)\,V(u,v) \quad (4)$$

The inverse Fourier transform of the measured visibility $V'(u,v)$ produces a degraded representation of the true brightness distribution of the source, commonly called dirty image, denoted by $I^D(x,y)$. The dirty image of the observed source $I(x,y)$ is then given by:

$$I^D(x,y) = \int S(u,v)V(u,v)e^{2\pi i(ux+vy)} dudv \quad (5)$$

In the classical image restoration theory, the dirty image is modeled by the convolution of the source image with the Point Spread Function (PSF) [6]. The PSF causes blurring in the source image resulting in a degraded image, the dirty image. Denoting by * the convolution operator and *B*, the PSF, this convolution is expressed as:

$$I^D(x,y) = I(x,y) * B(x,y) \quad (6)$$

In order to find what would be the PSF in a radiointerferometric array, the integral in eqn. (5) can be split into two parts using the Fourier transform properties:

$$I^D(x,y) = \int V(u,v)e^{2\pi i(ux+vy)} dudv * \int S(u,v)e^{2\pi i(ux+vy)} dudv \quad (7)$$

Considering eqn. (7), it can be noted that the first integral corresponds to $I(x,y)$, the Fourier inversion of $V(u,v)$, given by eqn. (1), and the second integral, to the PSF. Therefore, the PSF is:

$$B(x,y) = \int S(u,v)e^{2\pi i(ux+vy)} dudv \quad (8)$$

The radio interferometer image synthesis process is then reduced to a classical image restoration problem, and the PSF is called synthesized beam or dirty beam. In radio astronomy this problem is usually solved by standard deconvolution techniques, as the CLEAN [7] and the Maximum Entropy Method (MEM) [8].

## 3. CONFIGURATION DESIGN ASPECTS

The problem of optimizing the array configuration of a radio interferometer is to define the locations of the antennas in order to optimize the response function according to some specific criterion of image fidelity. Several approaches have been proposed to optimize the response of the array [1-3]. In generic interferometers, best imaging performance is achieved when the sampling in the Fourier domain is more uniform inside a circular boundary defined by the spatial resolution of the array [1]. A more uniform sampling in the Fourier plane provides images that are less affected by errors caused by the non-sampled Fourier components. However, the optimization of the positioning of the antennas involves several others aspects, that may be conflicting, such as cost or geographic constraints and specific requirements of the scientific goals.

This work proposes a new optimization strategy for the array configuration that is based on the entropy of the response function in both the Fourier and spatial domains. An ideal radio interferometer would yield a uniform distribution of sampled points in the Fourier domain and a point response for a point source in the reconstructed image. A stochastic optimizer, the Ant Colony System (ACS), employs the entropy of the reconstructed image and the entropy of the image in the Fourier domain to iteratively refine the array configuration. This strategy was developed in order to find some possible array configurations for the Brazilian Decimetric Array (BDA) [9], a radio interferometer that is currently being implemented to investigate solar phenomena.

The BDA is a radio interferometer operating in the frequency range of 1.2-1.7, 2.8 and 5.6 GHz with high spatial resolution of 4.5" at 5.6 GHz, and high temporal resolution, 100 ms. The BDA is intended to produce images of radio sources with high dynamic range [10-12]. It is being developed at the National Institute for Space Research (INPE, Brazil) as an international collaborative program. The images of active regions of the Sun provided by BDA will be analyzed by means of spectral tomography techniques. The scientific goal is to collect Solar images to be employed for space weather forecasting [13]. In addition, analysis of Solar flare components will lead to better understanding of fundamental problems in Solar Physics. BDA also will be useful for galactic and extra-galactic investigations of the Southern sky, which is not accessible by the Very Large Array (VLA) [14].

The BDA is being constructed at the INPE campus in Cachoeira Paulista, located approximately 110 km northeast of the main campus at São José dos Campos, Brazil. This site has a small valley of approximately 400m x 300m that was chosen for the radio interferometer. The antennas will be placed composing a central compact-T array. A control room with facilities to have on line data processing is already operational. The BDA project is being developed in three phases, described as follows. Each phase presents a specific design requirement, which implies a different optimization problem. The current work aimed at BDA phase II.

### 3.1. BDA Development Phases

In BDA phase I, 5 antennas are operated since the end of 2004. This prototype employs antennas with 4-meter diameter parabolic dish, elevation-azimuth mount and complete tracking capability and operating frequency range is 1.2–1.7 GHz [15]. The 5 antennas had been laid out over a distance of 216 meters in the West-East direction for a spatial resolution of about ~3 minutes of arc at 1.5 GHz. The aim of the prototype is to evaluate engineering aspects of the BDA system and to estimate the total cost of the project. This prototype will also allow the first Solar observations providing one dimensional profiles of the Sun with spatial and time resolutions of 3 min of arc and ~100 ms respectively.

In BDA phase II, it is planned to laid out 21 antennas over the distance of ~400 meters in the East-West direction and another 10 antennas over a distance of ~200 meters in the North-South direction forming a T-shaped array. The operating frequencies will include higher values: 1.2-1.7, 2.8 and 5.6 GHz. The major characteristics of the BDA phase II are shown in Table 1.

Finally, in BDA phase III, 4 more antennas will be added in the East-West direction and 2 more antennas in the Norht-South direction. The baselines will be increased in both directions to 2.5 km and 1.25 km, respectively, to increase the spatial resolution of the array up to approximately ~4.5 arc seconds at 5.6 GHz.

Table 1. Major parameters of BDA phase II.

| | |
|---|---|
| Observing frequency | 1.2-1.7 and 2.8 GHz |
| Field of View | 40’ |
| Spatial Resolution | 0.9’ |
| Temporal Resolution | 100 ms |
| Sensitivity | ~ 5 Jy |
| Numbers of Antennas | 31 |

## 4. ANT COLONY SYSTEM

This work proposes a new optimization strategy for the array configuration that is based on the entropy of the response function of the array in both the Fourier and spatial domains. The inverse design problem is formulated as an optimization problem [16] and is iteratively solved by a stochastic optimizer, the Ant Colony System (ACS).

The Ant Colony System (ACS) is a method that employs a metaheuristic approach based on the collective behavior of ants choosing a path between the nest and the food source [17]. Each ant marks its path with an amount of pheromone and the marked path is further employed by other ants as a reference. As an example of this, the sequence in Figure 1 shows how ants, trying to go from point A to point E (Figure 1a), behave when an obstacle is put in the middle of the original path, blocking the flow of the ants between points B and D (Figure

1b). Two new paths are then possible, either going to the left of the obstacle (point H) or to the right (point C). The shortest path causes a greater amount of pheromone to be deposited by the preceding ants and thus more and more ants choose this path (Figure 1c). The behavior of the ants represented schematically in Figure 1 is then used for the formulation and solution of an optimization problem.

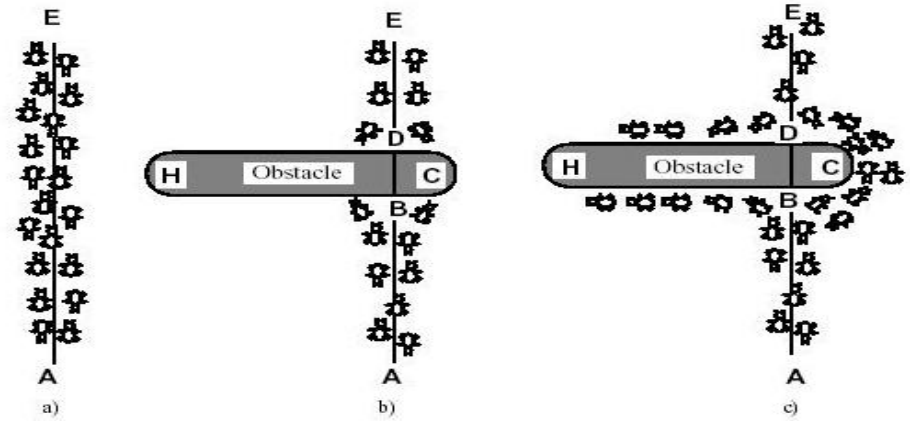


Figure 1. Ants overcoming an obstacle in the trail (from Dorigo *et al*. [17]).

In the ACS optimization method, several generations of ants are produced. For each generation, a fixed amount of ants (*na*) is evaluated. Each ant is associated to a feasible path that represents a candidate solution, being composed of a particular set of edges of the graph that contains all possible solutions. Each candidate solution is composed of a set of values, one for each unknown. This approach was successfully used for the Traveling Salesman Problem (TSP) and other graph like problems [18]. The best ant of each generation is then chosen and it is allowed to mark with pheromone its path. This will influence the creation of ants in further generations. The pheromone put by the ants decays according to an evaporation rate $\phi_{decay}$. Finally, at the end of all generations, the best solution is assumed to be achieved.

In this problem, the set of unknowns corresponds to the *X* and *Y* coordinates of the 31 antennas in the plane of the array. Therefore, there are *62* unknowns to be chosen on a probabilistic basis. The range for the *X* or *Y* coordinates is discretized in *np = 400* values. This approach was developed in order to deal with real valued unknowns**.** Each coordinate is considered to be one of the *ns=62* nodes of the graph. A particular solution $\chi$ is associated to the chosen values of the *62* coordinates linked pairwise by the edges, as schematically shown in Figure 2. Particularly, this figure depicts three paths, each one traversed by an ant. The maximum discretized value corresponds to the maximum baseline in meters of the desired final array.

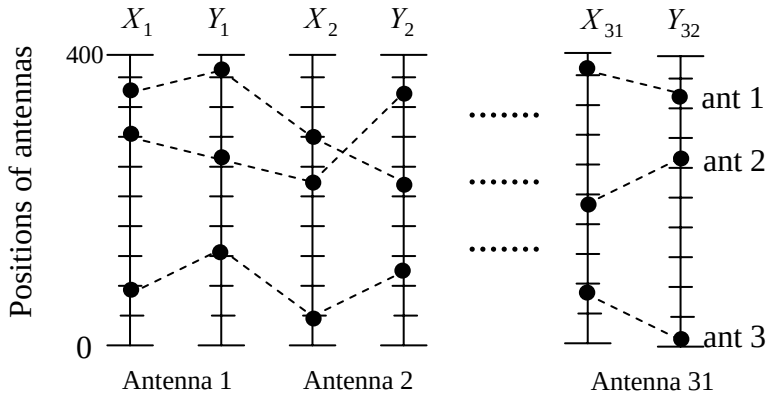


Figure 2. Schematical representation of the random generation of three ants associated to an array configuration. X and Y are unknown positions of antennas in the plane of the array.

As showed in Figure 5, a solution is composed of *ns* values, each one being a specific coordinate that is part of the candidate solution; for each coordinate, one out of *np* discrete values can be chosen. Therefore, all possible discrete values of the unknowns can be represented by an array *[i,j]* with *i = 1, 2, …, ns* and *j = 1, 2, …, np*, being therefore *ns* × *np* possible choices for the coordinates available. Another array with the same dimensions, $\phi_{ij}^{k}$ stores the amount of pheromone associated to the paths traversed by the best ants of every

generation. At the beginning, generation $k = 0$, all elements of the array $\phi_{ij}^{k}$ are assigned the following concentration of the pheromone $\phi_{ij}^{k=0} = \phi_0$. This amount is calculated as suggested in [19], using an evaluation $J(\chi)$ of eqn. (13), the objective function, obtained with a greedy heuristics:

$$\phi_0 = 1/(ns * J(\chi)) \tag{9}$$

The best ant in a given generation is allowed to mark its path, i.e. the corresponding elements of $\phi_{ij}^{k}$, with the maximum amount of pheromone, and this will have an influence on the generation of the ants in the following generation. For a given generation k, the amount of pheromone is given by

$$\phi_{ij}^{k} = (1 - \phi_{decay})\phi_{ij}^{k-1} + \delta_{ij,best}^{k-1}\,\phi_0 \tag{10}$$

where $\phi_{decay}$ is a value in the range $(0,1)$ and $\delta_{ij,best}^{k-1}$ is the Krönecker delta function associated with the path traversed by the best ant in the preceding generation $(k-1)$, i.e. the one which yields the best value for the objective function.

In an ACS, the probability of a given path $[i,j]$ to be chosen in generation $k$ is defined as [17]:

$$P_{ij}^{k} = \frac{\left[\phi_{ij}^{k}\right]^{\alpha}\left[\eta_{ij}\right]^{\beta}}{\sum_{l}\left\{\left[\phi_{il}^{k}\right]^{\alpha}\left[\eta_{il}\right]^{\beta}\right\}} \tag{11}$$

where $l \in [1,np]$ and $\eta_{ij}$ is the visibility/cost of each path, a concept that arises from the TSP, where the cost is the inverse of the distance of a particular path. Equation (11) assumes that all paths are possible for any ant, but particularly the TSP does not allow this assumption. The parameters $\alpha$ and $\beta$ are weights that establish the tradeoff between the influence of the pheromone and the visibility in the probability of each path.

However, there is a further scheme for the choice of a path for a new ant. According to a roulette, a random number in the range [0,1] is generated for the new ant and it is compared with a parameter $q_0$ chosen for the problem. If the random number is greater than this parameter, the path is taken according to $P_{ij}$. If not, the most marked path is assigned.

In the iterative optimization procedure, successive generations of ants are evaluated. Each ant is evaluated by means of an objective function that is related to the design goals of the radio interferometer. In this case, the value of the objective function $J(\chi)$ is given by the entropy of the distribution of sampled points in the Fourier domain for the candidate solution $\chi$. The visibility $\eta_{ij}$ information is not directly available for this problem, but a recent scheme, proposed and successfully employed in some inverse problems [20,21], allows imbedding visibility information in the ACS algorithm. This scheme uses a specific criterion to pre-select the ants in each generation. In this case, the chosen criterion was to select candidate solutions $\chi$ that present lower values of entropy for the corresponding PSF. There is a further advantage in the pre-selection since it reduces the amount of required evaluations in each generation. This has a strong impact on the computational performance.

## 5. STRATEGY FOR OPTIMIZATION

The optimization problem associated to the design of radio interferometric arrays consists to find antenna locations, constrained by the available terrain boundaries, in order to optimize the response function according to some specific criterion of image fidelity. Here, the proposed strategy is to obtain a more complete and uniform *uv* coverage. The measured visibility $V'(u,v)$ is defined by coverage and a corresponding PSF beam with a narrow main lobe and minimum intensity side lobes. An ideal radio interferometer would yield a complete and uniform distribution of sampled points in the Fourier domain. It would also present a PSF that is a Dirac delta function. Using entropy to evaluate these features, an optimized array configuration would maximize the entropy of the *uv* coverage and minimize the entropy of the PSF.

The BDA is being designed to obtain optimized images of radio sources at the decimetric band with high temporal and spatial resolutions. This precludes the use of Earth rotation synthesis [4] thus requiring an instantaneous image acquisition. The BDA uses a T-shape configuration that is more suitable considering site constraints and also implementation and maintenance costs [16]. In order to provide more flexibility in the choice of the array configuration, the T-shaped array was allowed to include antennas slightly displaced in the transverse direction, considering each baseline.

This work assumes that the radio source is located at the zenith, as in similar works found in the literature. For a generic pair of antennas $A_i$ and $A_j$ located at coordinates $(x_i, y_i)$ and $(x_j, y_j)$ respectively, the *uv* coverage is given by:

$$(u_{ij}, v_{ij}) = (x_i - x_j, y_i - y_j) \tag{12}$$

where $i \neq j$ and $i, j = 1,2,..., N_{tot}$, with $N_{tot}$ is equal to the numbers of antennas.

An Ant Colony based algorithm uses the entropy of the PSF to pre-select ants of a given generation, and employs an objective function given by the entropy of the *uv* coverage to refine the array configuration. At each iteration, a fixed amount of ants is then generated, pre-selected and evaluated, as described in Figure 3. Each ant corresponds to a candidate array configuration.

**5.1 Objective Function**

Each candidate solution $\chi$ is composed of the coordinates of the 31 antennas. The corresponding *uv* coverage is calculated from eqn. (12) and defines a bi-dimensional discrete probability density function (*F*). The objective function to be maximized is given by the entropy of *F*, given by:

$$J(\chi) = \sum_m \sum_n q_{mn} \log(q_{mn}) \quad \text{with} \quad q_{mn} = \frac{F_{mn}}{\sum_i \sum_j F_{ij}} \tag{13}$$

where *m* and *n* (or *i* and *j*) are indices of the rectangular grid associated to *F* in the Fourier plane. The entropy function above has its maximum value when the probability density function is uniform.

**5.2 Pre-selection of the Ants**

At each generation, a pre-selection is performed to select the ants that present the better PSF (*B*). Consequently, only a fraction of the generated ants is actually evaluated. The criterion adopted in the pre-selection is to obtain a PSF that presents a narrow and high intensity main lobe and side lobes with low intensity. Thus, the pre-selection function can also be done based on the entropy function of the PSF that has a minimum when *B* is the Dirac delta function. For each solution $\chi$, its PSF is calculated from eqn. (8) from its *uv* coverage. A fraction of the solutions is then selected based on the PSF entropy, given by:

$$J'(\chi) = \sum_m \sum_n q'_{mn} \log(q'_{mn}) \quad \text{with} \quad q'_{mn} = \frac{B_{mn}}{\sum_i \sum_j B_{ij}} \tag{14}$$

where *m* and *n* (or *i* and *j*) are indices of the rectangular grid associated to the PSF (*B*) in the space domain. A fraction of the candidate solutions with lower PSF entropy is selected and then evaluated by the eqn.(13).

```
♦ Initialization of the ACS parameters (e.g. NA, MIT, NS and NP)
♦ FOR each generation
     • FOR i = 1, NA (number of ants)
          - Generate each candidate solution χ by eqn.(11)
          - calculate the value of the pre-selection function by eqn.(14)
     • END FOR
     • Pre-select a fraction of the ants
     • Perform evaluation the selected ants by eqn.(13)
     • Select best ant and mark path with pheromone using eqn.(10)
♦ END FOR
```

Figure 3. Description of the optimization strategy.

**6. CONFIGURATION RESULTS**

In order to evaluate the proposed methodology, the T-shaped array of the BDA, composed of 31 antennas was also optimized by a standard approach, the geometric increasing spacing. It is based on the use of some multiples of a fundamental spacing b (in this case, b=9m), in such a way that the spacing between antennas is b or a power of 2 multiple (2b, 4b and 8b) along each arm of the T, as shown in Figure 4. No optimization algorithm was required.

Note that near the intersection of the East-West and North-South baselines, an uniform spacing equal to b is adopted. The maximum baseline is 378 m in East-West direction and 189 m in North-South direction respectively. The correspondent *uv* coverage and synthesized beam pattern are shown in Figures 5a and 5b. The *uv* plane presents a good coverage in the low frequencies due to the large number of antennas located near to the

intersection of the T, with uniform spacing of 9 m. The side lobes are minimized below 25% of the intensity of the main lobe in the dirty image.

Then, the 31 antenna positions were optimized using the proposed strategy. The T-shape array was adopted, but antenna positions were allowed to be along each baseline with a degree of freedom in the transverse direction. The maximum transverse shift was imposed as being 20% of the length of the respective baseline**.**

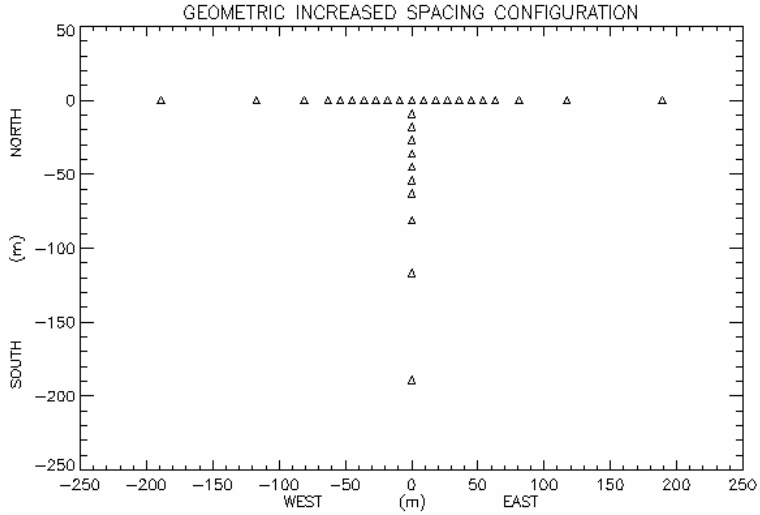


Figure 4. T shape array with 31 antennas using a geometric-increased spacing (each antenna is represented by a small triangle).

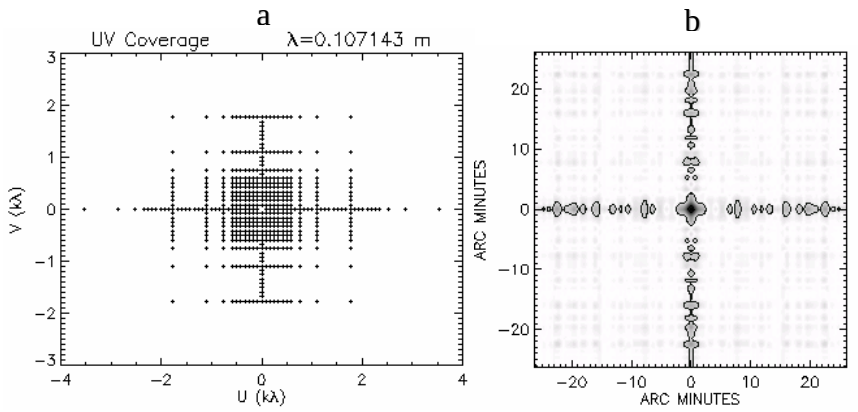


Figure 5. Resulting *uv* coverage (a) and synthesized beam (b) obtained for the geometric increased spacing configuration.

The current implementation required the usual adjustment of the ACS parameters like $\rho$ and $q_0$. The values of $\alpha$ and $\beta$ were not required as visibility was taken into account in the referred pre-selection. Similarly, to other stochastic optimization algorithms, in the ACS, the tuning of these parameters is decisive. Other parameters may influence the quality of the solution, like the range of discretization for the *np* possible paths between each pair of the *ns* nodes, the number of ants *na* or the maximum number of iterations *mit*. The ACS optimizer of this work employs the values shown in Table 2. The *ns* parameter is the number of independent coordinates *(x,y)* of the 31 antennas that compose the BDA. The parameter *np* is related to discrete positions in meters that are possible for each coordinate. The ACS employed 100 ants in each generation and the total number of generations/iterations is 400.

Table 2. Ant Colony System parameters.

| *ns* | *np* | *na* | *mit* | $\rho$ | $q_0$ |
|---|---|---|---|---|---|
| 62 | 400 | 100 | 400 | 0.03 | 0.0 |

The optimized configuration is shown in Figure 6 and the resulting *uv* coverage and the synthesized beam, in Figures 7a and 7b, respectively. The maximum baselines of the array are 400 m in the East-West direction and 200 m in the North-South direction.

The flexibility in the geometry of the T-shaped array with transverse displacement of the optimized configuration allowed the ACS to obtain a configuration with a more complete and uniform distribution of sampled points in the Fourier plane with less redundancy, as shown in the Figure 7a. This reduces the side lobes caused by missing points in the *uv* plane. Figure 5b shows that the side lobes are minimized below ~20% of the intensity of the main lobe. In addition, this configuration is less susceptible to errors due to unmeasured components in the Fourier plane.

On the other hand, the geometric-increased spacing yields a configuration that presents a more dense array near the intersection of the T, where the antennas are placed at intervals of 9 meters. This configuration also presents a high degree of redundant points in the Fourier Plane, that implies less measured points and consequently more gaps in the *uv* plane. Assuming perfect visibility data, the effect of the missing *uv* points yields side lobes with intensities below 25% of that of the main lobe.

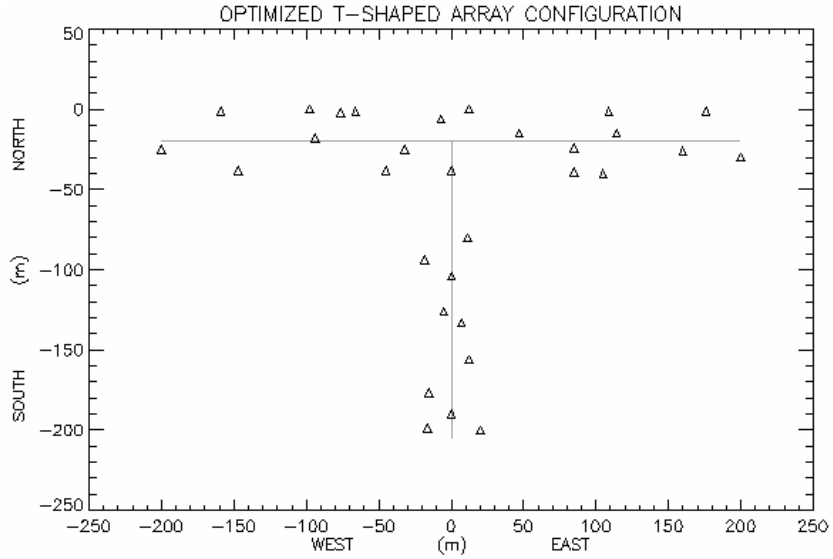


Figure 6. Optimized configuration obtained with 31 antennas using optimized spacing strategy (each antenna is represented by a small triangle).

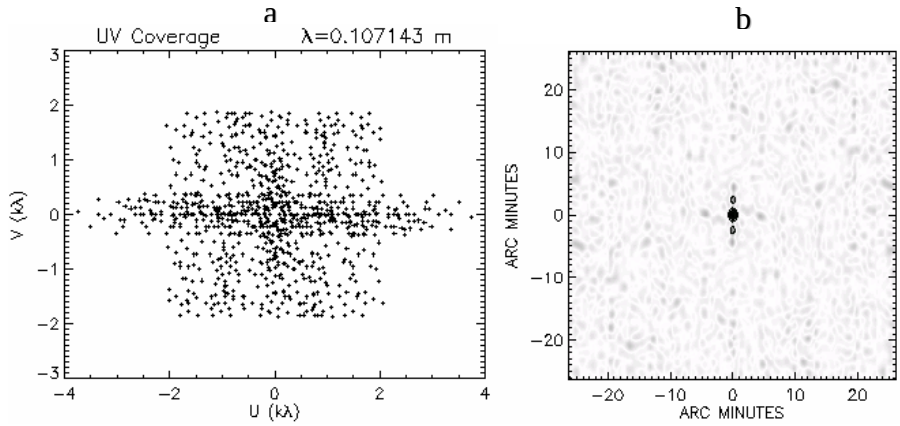


Figure 7. Resulting *uv* coverage (a) and synthesized beam (b) obtained for the optimized configuration.

In order to investigate the quality of the *uv* coverage of the optimized configuration on the radio imaging of the Sun, a simulation was performed using input data acquired by the Nobeyama Radio Heliograph [22] at 17 GHz as a model of the source (Figure 8a). In this simulation, the position of the source is assumed located at the zenith and the observation frequency is 2.8 GHz. The resulting dirty image is shown in Figure 8b. It was obtained performing the following steps:

1. Application of a Discrete Fourier Transform (DFT) in the source image to obtain the discrete visibility function *V(u,v)*;
2. Computation of the sampling function *S(u,v)* in the Fourier plane for the optimized array configuration, using the eqn.(3).
3. Sampling the visibility function *V(u,v)* using *S(u,v)* producing the sampled visibilities *V'(u,v)*;
4. Inverse Fourier transformation of the *V'(u,v)* to obtain the dirty image of the source.

In the radio imaging of the Sun, the optimized configuration produced a dirty image with information about the small structures in the Sun, as well as, presented information about the contour of the Solar disc (Figure 6b), while the optimized configuration presents some distortions in small structures due to a lack of highest baselines in the geometric increased spacing configuration..

In the simulations, a uniform weighting was chosen for the *uv* coverage. In real image acquisition, weighting is not uniform, due to the tapering effect, and the level of side lobes is further reduced.

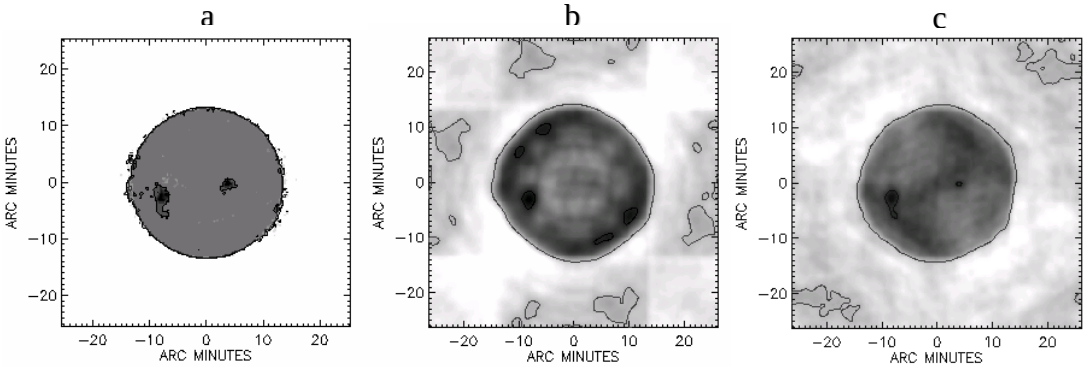


Figure 8. (a) Image of Solar disc obtained from Nobeyama Radio Heliograph at 17 GHz that was used as a model of the Sun; (b) dirty image simulated using the geometric-increased spacing and (c) dirty image simulated using the optimized configuration.

In this simulation of radio imaging of the Sun, the configuration based on the geometric increased spacing produced a dirty image that presents degraded information about small structures in the Sun. However, large structures, like the Solar disc and bigger active regions can be detected, as seen in Figure 8b. The optimized configuration presents better quality in both the small and large structures in the Sun (Figure 8c). The corresponding dirty image presents some distortion, that is due to the incomplete *uv* coverage that is inherent to this problem.

## 7. FINAL COMMENTS

The current work presents a new strategy for choosing antenna locations of radio interferometric arrays. The optimization of the array is based on the entropy of the response function of the array in both the Fourier and spatial domains. A stochastic algorithm, the Ant Colony System, was chosen to iteratively optimize the array configuration. Each ant of a generation corresponds to a candidate solution that is evaluated by an objective function based on the entropy of the sampled visibilities *V'(u,v)* in the Fourier domain. In addition, ants are pre-selected based on the entropy of the PSF.

Particularly, the present investigation was focused on searching antenna positions for a T-shaped array with the antennas having the flexibility of being placed slightly outside the arms of the T, in a transversal direction. This restriction is due to construction and operational aspects. The proposed strategy converges to an array configuration that provides a more uniform and complete *uv* coverage *V'(u,v)* with less redundancy, in comparison to a standard optimization scheme. There is also a reduction of the side lobes in the dirty image, since there are less missing *uv* points. This makes the optimized configuration less susceptible to errors due to the unmeasured components in the Fourier plane. Furthermore, the corresponding beam has a narrower main lobe and minimum intensity side lobes.

A simulation of the solar imaging process was performed for the optimized array using data from the Nobeyama Radio Heliograph. The entire imaging process was reproduced in order to see the dirty image that would be generated for that array. The resulting solar image has good quality, allowing identification of the Solar disc and also structures in the Solar surface.

## REFERENCES

1. E. Keto, The shapes of cross-correlation interferometers. *Astrophysical J.* (1997) **475**, 843-852.
2. T. J. Cornwell, A novel principle for optimization of the instantaneous fourier plane coverage of correlation arrays. *IEEE Trans. Antenna Propag.* (1988) **36**, 1165–1167.
3. L. Kogan, Optimizing a large array configuration to minimize the sidelobe. *IEEE Trans. Antenna Propag.* (2000) **48**, 1075-1078.
4. A. R. Thompson, J. M. Moran and G.W. Swenson Jr., *Interferometry and Synthesis in Radio Astronomy,* Wiley, New York, 1986.

5. R. Wohlenben, H. Mattes and Th. Krichbaum, *Interferometry in Radioastronomy and Radar Techniques*, Kluwer, Dordrecht, 1991.

6. R. C. Gonzalez and R.E. Woods, *Digital Image Processing,* Addison-Wesley, Reading, Massachusetts, 1988.

7. J. Högbom, Aperture synthesis with a non-regular distribution of interferometer baselines. *Astronomy and Astrophysics Suppl.* (1974) **15**, 417-426.

8. R. Narayan and R. Nityananda, Maximum entropy image restoration in astronomy. *Ann. Rev. Astronomy and Astrophysics* (1986*)* **24**, 127-170.

9. H. S. Sawant, K.R. Subramanian, E. Lüdke, J. H. A. Sobral, G. Swarup, F. C. R. Fernandes, R. R. Rosa and J. R. Cecatto, Brazilian decimetric array. *Adv. Space Res*. (2000) **25**(9), 1809-1812.

10. H. S. Sawant, J. A. C. F. Neri, F. C. R. Fernandes, J. R. Cecatto, M. R. Sankararaman, M. B. Alonso, E. Ludke, G. Swarup, S. K. Ananthkrishnan and K. R. Subramanian, A low cost steerable radio-telescope. *Adv. Space Res.* (2003) **32**(12), 2715-2720.

11. H. S. Sawant, F. C. R. Fernandes, J. A. C. F. Neri, J. R. Cecatto, C. Faria, S. Stephany, R. R. Rosa, M. C. Andrade, E. Ludke, K. R. Subramanian, R. Ramesh, M. S. Sundrarajan, M. R. Sankararaman, S. Ananthakrishnan, G. Swarup, J. W. V. Boas, L. C. L. Botti, C. E. Moron, J. H. Saito and M. Karlický, Southern hemisphere solar radio heliograph, *Proc.10th European Solar Physics Meeting, ESA SP-506*, Noordwijk, The Netherlands, 2002, Vol. **2**, pp.971-974.

12. H. S. Sawant, E. Ludke, K. R. Subramanian, J. R. Cecatto, F. C. R. Fernandes, R. R. Rosa, J. H. A. Sobral, E. Scalise Jr., J. W. V. Boas and L. C. L. Botti, A high resolution decimetric solar radio heliograph. *Astronomical Soc. Pacific Conf. Ser.* (2000) **206**, 341-346.

13. K. Marubashi, The space weather forecast program. *Space Sci. Rev.* (1989) **51**, 197-214.

14. A. R. Thompson, B. G. Clark, C. M. Wade and P. J. Napier, The very large array. *Astronomical J. Suppl.* (1980) **44**, 151-167.

15. J. R. Cecatto, F. C. R. Fernandes, J. A. C. F. Neri, N. Bethi, N. S. Felipini, F. R. H. Madsen, M. C. Andrade, A. C. Soares, E. M. B. Alonso and H. S. Sawant, Prototype of the first Brazilian interferometer, the Brazilian decimetric array project. *SAB (Brazilian Astronomical Soc.) Bulletin* (2004), **23**(3), 25-38.

16. C. Faria, H. S. Sawant and S. Stephany, Solar radio observations with high spatial resolution, *Proc. IV Workshop of the Applied Computing Post-graduate Program (IV WORCAP)*, S. José dos Campos, Brazil, 20-21 October, 2004 (in CD-Rom).

17. M. Dorigo, V. Maniezzo and A. Colorni, The ant system: optimization by a colony of cooperating agents. *IEEE Trans. on Systems, Man, and Cybernetics – Part B* (1996) **26**(2), 29-41.

18. J. C. Becceneri and A. S. I. Zinober, Extraction of energy in a nuclear reactor by ants, *Proc. XXIII Brazilian Symposium on Operations Research,* Campos do Jordão, Brazil, 06-09 November, 2001.

19. E. Bonabeau, M. Dorigo and G. Theraulaz, *Swarm Intelligence: From Natural to Artifical Systems,* Oxford University Press, London, 1999.

20. A. J. Preto, H. F. Campos Velho, J. C. Becceneri, M. Fabbri, N. N. Arai, R. P. Souto and S. Stephany, A new regularization technique for an ant-colony based inverse solver applied to a crystal growth problem, *Proc. 13th Inverse Problems in Engineering Seminar (IPES-2004)*, Cincinnati, 14-15 June, 2004, pp.147-153.

21. R. P. Souto, H. F. C. Velho, S. Stephany and S. Sandri, Reconstruction of chlorophyll concentration profile in offshore ocean water using ant colony system, *Proc. First Hybrid Metaheuristics (HM-2004),* Valencia, Spain, 22-23 August, 2004, pp.19-24.

22. H. Nakajima, M. Nishio, S. Enome, K. Shibasaki, T. Takano, Y. Hanaoka, C. Torii, H. Sekiguchi, T. Bushimata, S. Kawashima, N. Shinohara, Y. Irimajiri, H. Koshiishi, T. Kosugi, Y. Shiomi, M. Sawa and K. Kai, The Nobeyama radioheliograph. *Proc. IEEE* (1994) **82**(5), 705-713.